Letter

# Coherence transfer in quantum networks

Chun-Yang Lin, Yu-Cheng Li, Shih-Hsuan Chen, Sheng-Yan Sun, Ching-Jui Huang, Kuan-Jou Wang, and Che-Ming Li*

*Department of Engineering Science, National Cheng Kung University, Tainan 70101, Taiwan*
*and Center for Quantum Frontiers of Research & Technology, National Cheng Kung University, Tainan 70101, Taiwan*

(Received 24 April 2026; accepted 2 November 2026; published 18 November 2026)

Detecting coherence transfer in complex quantum networks is challenging under uncharacterized experimental conditions and with limited access to the system. Here, we use the coexistence of static and dynamic coherence to derive a nonlinear criterion for coherence transfer. The criterion applies even when the verification capabilities of checkpoint nodes are uncharacterized. It requires only minimal one-network output analysis, up to the number of output state dimensions. Each output requires only two-setting measurements of state populations, regardless of the network size. The criterion is general for both spatial and temporal networks, including those with multiple coherence sources, and applies to quantum transport in solid-state nanostructures. Experimentally, using entanglement swapping, we transfer polarization-entangled pairs in four- and six-photon entanglement networks. The criterion provides experimental evidence of coherence transfer in multiphoton entanglement networks. Our findings provide a practical tool for investigating the presence, role, or function of coherence transfer in quantum networks.

DOI: 10.1103/lv5x-mvvh

*Introduction.* Quantum networks [1,2] are essential for exploring how quantum states transfer between diverse systems to enable nonclassical functions, from naturally occurring *in vivo* energy transport [3] to the engineering of a world clock [4], and from chip-scale requirements in quantum computers [5] to applications across the large-scale quantum internet [6,7]. A key feature is their ability to transfer quantum coherence between network nodes, a phenomenon classical physics cannot explain [8]. This process relies on establishing and maintaining quantum coherence [9–11] and becomes a vital aspect of quantum networks as quantum techniques advance [12].

Verifying coherence transfer in action, whether in biological [13] or artificial [14,15] systems, is challenging due to two experimental constraints: (1) uncharacterized experimental conditions and (2) restricted system access. Experimental trust issues stem from environmental noise and experimental flaws, causing a node's actual state to deviate from expectations, as in long-distance communication networks [16,17]. A node and its associated manipulations are considered uncharacterized when insufficient information exists about the noise and flaws. Access issues involve measuring or controlling the network and its components. Because a node's degrees of freedom may permit only basic or indirect measurements given the limited available techniques, this limited access leads to an incomplete understanding of networks, for example, quantum process tomography of charge transport through nanostructures using only available charge detection [18] and of the transfer of electronic excitations in a photosynthetic complex [19] using two-dimensional electronic spectroscopy (2DES) [20].

Progress has been made in understanding coherence [8,21], but confirming its transfer under both constraints remains difficult. While theories involving quantum operations, such as quantum channel resources [9,10] and quantum process capability [11], analyze coherence, they require known quantum state and process tomography, which conflicts with constraints (1) and (2). Quantum coherence witnesses [22,23] can verify the quantum nature under constraint (2) but are incompatible with constraint (1) because they require measurements of propagators conditioned on precise state preparation and time control. Although the robustness of coherence witnesses [24–28] simplifies experiments, measurement errors can still affect their accuracy. They may help under constraint (2) but are vulnerable under constraint (1), depending on measurement precision. Testing the Leggett-Garg inequality [29,30] can reveal quantum dynamics such as coherence creation or preservation under constraint (1). It requires noninvasive measurements, making practical application under constraint (2) difficult. Measurement-device-independent qubit coherence methods [31] using tomography have been proposed for untrusted devices, potentially addressing constraint (1). However, they are limited by constraint (2) due to their reliance on tomography. Recently, quantum coherence in triangular networks with independent sources and joint measurements was demonstrated without adjustments [32]. While partially addressing constraints (1) and (2), their scope is limited to these specific structures and does not cover broader constraints.

This work has a twofold goal. First, we introduce a practical and general coherence-transfer criterion that

*Contact author: cmli@mail.ncku.edu.tw

*Published by the American Physical Society under the terms of the Creative Commons Attribution 4.0 International license. Further distribution of this work must maintain attribution to the author(s) and the published article's title, journal citation, and DOI.*

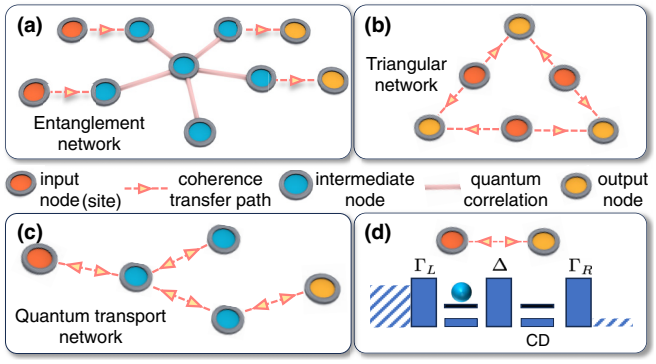



FIG. 1. Coherence transfer in quantum networks. The coherence-transfer criterion (1) and its temporal analog (3) apply across various access levels and scenarios, including (a) entanglement networks [33,34], as demonstrated in our experiments; (b) the triangular network with three coherence sources [32], where each input node emits a single particle in a superposition of two paths toward the output nodes; (c) quantum transport networks [18], such as single-charge transport between sites (nodes) in nanostructures; and (d) a double quantum dot [14] serving as a primitive unit, with charge detectors (CDs) used for measurement.

accommodates the experimental constraints (1) and (2). The criterion works under constraint (1) for nodes with unknown detection capabilities and, under constraint (2), requires only two measurement settings, irrespective of network size, for a minimal one-network output analysis, up to the number of output state dimensions. These two features make the criterion broadly applicable across various spatial and temporal coherence-transfer scenarios, including entanglement, multi-coherence sources, and quantum transport networks. Second, we apply this criterion to the transfer of qubits within four- and six-photon entanglement networks and experimentally detect their coherence, which cannot be achieved with known methods under the limited experimental constraints [9–11,22–32]. These results help ease the difficulties encountered in coherence-transfer experiments [3–7,13–20].

*Theory and methods.* Coherence transfer in networks, $\mathcal{E}_{\rm Net}$, involves three stages: input, evolution, and output, with nodes either entangled [33,34] or not [35]. The input process sets the coherence of the transfer state, $\rho_{{\rm in},k}$, at the input nodes, where $k$ labels the different states. During evolution, coherence propagates from the input through intermediate nodes to the output nodes. The output nodes then receive and output the state, $\rho_{{\rm out},k}$, with coherence for applications such as measurement-based quantum information in entanglement networks [36–38]. Figures 1(a)–1(c) illustrate the three stages across three scenarios.

We introduce a coherence-transfer detection access system, as shown in Fig. 2. The experimental network's output node (not shown) and a checkpoint node with a verifier serve as the user and the access control manager, respectively. The checkpoint node first assesses whether characterizing $\mathcal{E}_{\rm V}$ is feasible under the experimental constraints (1) and (2) and whether the output node can comply with the access policies and bear the cost of characterizing $\mathcal{E}_{\rm V}$ [39]. If characterizing $\mathcal{E}_{\rm V}$ is feasible and the output node can provide the required cost, the checkpoint node uses standard coherence measures

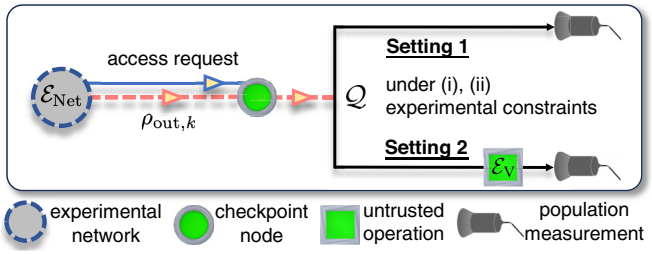



FIG. 2. Coherence-transfer detection access system. Once the checkpoint node approves the coherence-detection task from the network ($\mathcal{E}_{\rm Net}$), coherence-transfer detection determines $\mathcal{Q}$ [Eq. (1)] by first measuring the output-state population $\rho_{{\rm out},k}$ at the output checkpoint node (Setting 1) and then performing additional measurement rounds following an uncharacterized (untrusted) checkpoint operation $\mathcal{E}_{\rm V}$ (Setting 2).

(not shown in Fig. 2). Otherwise, the checkpoint node implements coherence detection using our introduced criterion [39].

The verifier at the checkpoint nodes can follow the procedure below to detect coherence transfer. First, the verifier measures $\rho_{{\rm out},k}$ to determine their *static* populations in the experimental state basis, $\{|i\rangle\} = \{|i\rangle | i = 0, 1, \ldots, d-1\}$, which form the diagonal matrix of the output states' density operator, $\rho^{\rm (d)}_{{\rm out},k}$ (Setting 1 in Fig. 2). Then, the verifier applies an operation, $\mathcal{E}_{\rm V}$, with an unknown *dynamic* ability to create coherence, on $\rho_{{\rm out},k}$. Next, the verifier measures them to determine their populations, assuming a faithful measurement (Setting 2 in Fig. 2). These populations are the probabilities of observing the basis states, $|i\rangle$ for the state $\mathcal{E}_{\rm V}(\rho_{{\rm out},k})$, denoted as $P_{\mathcal{E}_{\rm V}}(i|\rho_{{\rm out},k})$. Based on the experimental outcomes above, we identify a new property of coherence transfer that emerges only when both the output states of a network possess coherence and the operation applied to them can create coherence (dynamic coherence). With the coexistence of two coherences, we define our criterion for coherence transfer for the output states produced from the $n$ input-state types as a nonlinear form:

$$\mathcal{Q} := \min_{\mathcal{E}_{\mathcal{I}}} \sum_{k=1}^{n} \sum_{i=0}^{d-1} \left| P_{\mathcal{E}_{\rm V}}(i|\rho_{{\rm out},k}) - P_{\mathcal{E}_{\mathcal{I}}}\left(i|\rho^{\rm (d)}_{{\rm out},k}\right) \right| > 0, \quad (1)$$

where $P_{\mathcal{E}_{\mathcal{I}}}(i|\rho^{\rm (d)}_{{\rm out},k}) = {\rm tr}[|i\rangle\langle i|\mathcal{E}_{\mathcal{I}}(\rho^{\rm (d)}_{{\rm out},k})]$ and $\mathcal{E}_{\mathcal{I}}$ is a process that cannot generate coherence from any incoherent states [11,40]. The kernel $\mathcal{Q}$ is obtained by minimizing over all incapable processes and can be computed using semidefinite programming (SDP) [40–43].

When criterion (1) is satisfied, the process $\mathcal{E}_{\rm Net}$ is confirmed to transfer coherence effectively, and $\mathcal{E}_{\rm V}$ is recognized as capable of generating coherence. Its detection resolution depends primarily on the assumption of reliable population measurements and on the coherence properties of $\rho_{{\rm out},k}$ and $\mathcal{E}_{\rm V}$. The tightness, optimality, detection power, error in a measured $\mathcal{Q}$, and SDP numerical errors related to the kernel or criterion are detailed in Supplemental Material [40]. Because criterion (1) captures both the static coherence feature and the dynamic transfer property, it is comprehensive and suitable for a wide range of coherence network detection tasks under experimental constraints [44], compared with existing work

[9–11,22–32]. It is worth noting that when it is experimentally feasible to characterize and further calibrate $\mathcal{E}_{\mathrm{V}}$, it can be chosen to maximize the criterion based on $\mathcal{E}_{\mathrm{V}}$'s coherence-creation capability, thereby yielding the maximum value of $\mathcal{Q}$ [40].

To prove criterion (1), we use the operator-sum representation [45] to model $\mathcal{E}_{\mathrm{V}}$ acting on $\rho_{\mathrm{out},k} = \sum_{m,n=0}^{d-1} \rho_{k,mn} E_{mn}$, with $E_{mn} = |m\rangle\langle n|$, as $\mathcal{E}_{\mathrm{V}}(\rho_{\mathrm{out},k}) = \sum_{m,n,i,l=0}^{d-1} \chi_{mn,il} E_{mn} \rho_{\mathrm{out},k} E_{il}^{\dagger}$, where $\chi_{mn,il}$ is the process matrix of $\mathcal{E}_{\mathrm{V}}$ and describes the transition from the coherence terms $|n\rangle\langle l|$ to the diagonal elements $|m\rangle\langle m|$ when $m = i$ and $n \neq l$. Then, we have $P_{\mathcal{E}_{\mathrm{V}}}(i|\rho_{\mathrm{out},k}) = \sum_{n,l=0,n\neq l}^{d-1} \rho_{k,nl}\chi_{in,il} + \sum_{n=0}^{d-1} \rho_{k,nn}\chi_{in,in}$ and $P_{\mathcal{E}_{\mathcal{I}}}(i|\rho_{\mathrm{out},k}^{(\mathrm{d})}) = \sum_{n=0}^{d-1} \rho_{k,nn}\chi_{\mathcal{I},in,in}$, where $\chi_{\mathcal{I},in,in}$ is the process matrix element of $\mathcal{E}_{\mathcal{I}}$ [11]. These imply that $\mathcal{Q} = 0$ when $\rho_{k,nl} = 0$ and $n \neq l$ (the network process cannot generate coherence), or when $\chi_{in,il} = 0$ and $n \neq l$ (the verifier cannot produce coherence), or both conditions are met simultaneously. Therefore, $\mathcal{Q} > 0$ clearly indicates that the network process can transfer coherence and that $\mathcal{E}_{\mathrm{V}}$ can generate coherence, as described by Eq. (1) [46].

The two-setting-only criterion generally applies to scenarios where population measurements and an uncharacterized $\mathcal{E}_{\mathrm{V}}$ are available for analyzing sufficient network output states. It is summarized in the three groups below.

(G1) $n = 1$. When a network is defined within a specific, well-understood physical framework, $\mathcal{E}_{\mathcal{I}}$ can be directly described by that framework. That is, we require precise *a priori* knowledge of the network structure and the quantum-mechanical descriptions, as well as the physical assumptions underlying the absence of network coherence-transfer capability and the checkpoint's lack of coherence-creation capability. Together, these two requirements make $\mathcal{E}_{\mathcal{I}}$ explicitly suited to a concrete network, so minimizing the kernel $\mathcal{Q}$ is analytically feasible for defining the criterion's operational boundaries (1). The triangular network with three coherence sources [32] [Fig. 1(b)] is a concrete example that illustrates how these requirements make the $n = 1$ case applicable. To detect the coherence transfer of a joint state, $\rho_{\mathrm{out}}$, in the network generated when each input node emits a single particle in a superposition of two paths toward the output nodes, one can use a 50:50 beam splitter (BS) at each vertex of the triangle to interfere the two incoming modes, acting as the checkpoint operation $\mathcal{E}_{\mathrm{V}}$, and consider the following criterion:

$$\mathcal{Q} = \min_{\mathcal{E}_{\mathcal{I}}} \sum_{a,b,c=0}^{1} \left| P_{\mathcal{E}_{\mathrm{V}}}(a,b,c \mid \rho_{\mathrm{out}}) - P_{\mathcal{E}_{\mathcal{I}}}\left(a,b,c \mid \rho_{\mathrm{out}}^{(\mathrm{d})}\right) \right| > 0, \tag{2}$$

where $a$, $b$, and $c$ represent the binary postselected measurement results for each BS's two output modes. The kernel is analytically minimized by considering all incapable processes within a classical, realistic model that cannot yield coherence, thereby eliminating the need for an additional experiment to obtain $\rho_{\mathrm{out}}^{(\mathrm{d})}$. Therefore, $\mathcal{Q} > 0$ holds in this scenario, implying that coherence transfer can be detected without changing the state or modifying the local measurement setting [32]. See Supplemental Material for further discussion [40]. Compared with the existing detection method [32], criterion (2) identifies the role of BSs and shows that their operation can produce coherence. The conclusion above applies directly to networks with multiple vertices and coherence sources.

(G2) $n \geqslant 2$. In a broader context, when knowledge of the network is limited, $\mathcal{E}_{\mathcal{I}}$ is defined by its failure to achieve coherence within the general quantum operation formalism [11]. To be practical in these cases, as demonstrated experimentally below for entanglement networks, at least two distinct input and output state configurations are required ($n \geqslant 2$). See Supplemental Material [40] for a detailed discussion. (G3) Networks in the time domain. For an unknown dynamics $\mathcal{E}_{t,0}$ in an open quantum system coupled to a reservoir [50], criterion (1) has a temporal version that can be used to determine whether it can generate coherence in the state basis $\{|i\rangle\}$ over time, for example, in the site basis of quantum transport networks [Fig. 1(c)]. Initially, we consider $n$ states with different initial conditions at time 0, denoted by $\rho_{k,0}$, for $k = 1, 2, \ldots, n$. For each $k$, we perform population measurements at time $t_0$ on the states $\rho_{k,t_0}$ that have evolved under the dynamics $\mathcal{E}_{t_0,0}$ from time 0 to $t_0$. Subsequently, we also conduct population measurements at a later time $t$, where $t > t_0$, on the states $\rho_{k,t}$ that have evolved under the dynamics $\mathcal{E}_{t,0}$ from 0 to $t$. This includes the additional evolution from $t_0$ to $t$, which is described by the dynamics $\mathcal{E}_{t,t_0}$, corresponding to the role of $\mathcal{E}_{\mathrm{V}}$ in Eq. (1). We then determine the probability of observing the state $|i\rangle$ at time $t$: $P(i|\rho_{k,t})$, and the diagonal component of $\rho_{k,t_0}$: $\rho_{k,t_0}^{(\mathrm{d})}$. The temporal equivalent of criterion (1) states that

$$\mathcal{Q}_t := \min_{\mathcal{E}_{\mathcal{I}}} \sum_{k=1}^{n} \sum_{i=0}^{d-1} \left| P(i|\rho_{k,t}) - P_{\mathcal{E}_{\mathcal{I}}}\left(i|\rho_{k,t_0}^{(\mathrm{d})}\right) \right| > 0, \tag{3}$$

where $P_{\mathcal{E}_{\mathcal{I}}}(i|\rho_{k,t_0}^{(\mathrm{d})}) = \mathrm{tr}[|i\rangle\langle i|\mathcal{E}_{\mathcal{I}}(\rho_{k,t_0}^{(\mathrm{d})})]$. For systems coupled to the reservoir Markovianly [50], any dynamics that cannot produce coherent transitions between states in the basis $\{|i\rangle\}$ yield $\mathcal{Q}_t = 0$ [40]. When experimental results satisfy criterion (3), $\mathcal{E}_{t,0}$ is confirmed to generate coherence between states over time.

Criterion (3) shares the same advantages as criterion (1) in the time domain. First, compared with the most effective time-domain witness [22,23], our criterion is more practical because it does not require additional reliable reference states or propagator measurements. Second, the role of $\mathcal{E}_{\mathrm{V}}$ is played by the additional system dynamics from $t_0$ to $t$. This makes detection of coherence dynamics experimentally feasible using only population measurements. Using quantum transport in the Markovian limit as an example [Figs. 1(c) and 1(d)], coherence dynamics can be detected solely from site population measurements of single charges [Fig. 1(d)]. Finally, criterion (3) is highly sensitive. As shown in Fig. 3, it detects coherence in single-electron transport through a double quantum dot. Compared with the time periods identified by violations of the one-initial-state, three-time-point Leggett-Garg-type inequality [14] (which a classical Markovian system under noninvasive charge measurement satisfies), our criterion can detect a much broader window of quantum coherence, given three initial states ($n = 3$) for considering $\mathcal{Q}$ and implementing minimization via SDP, and within the same limits to which the master equation formalism applies [14]. This identifies coherence transfer through the coexistence of static and dynamic coherence, distinct from approaches that

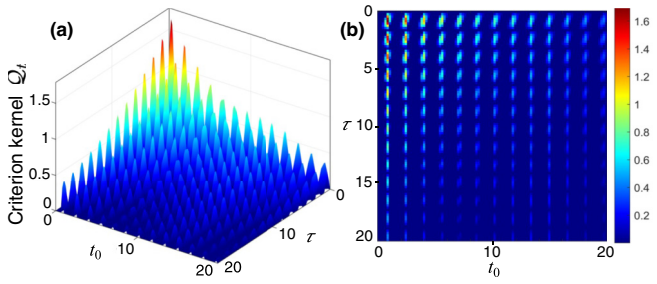



FIG. 3. Detecting coherence transfer in single-electron transport through a double quantum dot. For the setup in Fig. 1(d), we assume weak coupling, large bias, and Coulomb blockade, with CDs used for the measurements. The left and right tunneling rates and the coherent tunneling amplitude between the left and right dots are $\Gamma_L = 4$, $\Gamma_R = 0.1$, and $\Delta = 1$, respectively. (a) The nonvanishing $\mathcal{Q}_t$ indicates regions where coherence develops during quantum transport, as shown in its density plot [panel (b)], where $\tau = t - t_0$ is the time difference for Eq. (3). See Supplemental Material [40] for a detailed discussion, including the SDP complexity.

rule out a classical description of transport through a nanostructure using a Leggett-Garg-type inequality.

*Experiments.* Building on our previous results [51], we demonstrate that criterion (1) detects one- and two-qubit coherence transfer in four- and six-photon polarization-entanglement networks across four transmission scenarios. Two-qubit transfer involves inputting a Bell state and transferring it via a Bell-state measurement (BSM) [47,49] using wave plates, a polarizing beam splitter (PBS), and shared entanglement [see Fig. 4(a)]. In four-photon networks [Fig. 4(b)], coherence propagates from node 1 and node 3 to node 2 and node 4 through a single BSM. In six-photon networks [Fig. 4(c)], the coherence input occurs via a BSM from node 2 and node 5, assisted by the BSM of node 1 and node 3, to node 4 and node 6. This process can also be viewed as entanglement swapping [52,53] within a star six-photon entanglement network [Fig. 1(a)] using Bell states and BSMs. The effectiveness of coherence transfer, evaluated using $\mathcal{Q}$, is based on the basis $\{|i\rangle\} = \{|0\rangle = |HH\rangle, |1\rangle = |HV\rangle, |2\rangle = |VH\rangle, |3\rangle = |VV\rangle\}$. In each multiphoton entanglement network, we perform two coherence-transfer processes, $\mathcal{E}_{\mathrm{Net},1}$ and $\mathcal{E}_{\mathrm{Net},2}$, designed to be *capable* of achieving the target process above and *incapable* of creating coherence under postselection [40], respectively. The operations applied to output states at the checkpoint node $\mathcal{E}_{\mathrm{V1}}$, $\mathcal{E}_{\mathrm{V2}}$, and $\mathcal{E}_{\mathrm{V3}}$ correspond to quarter-wave plate (QWP) settings with the fast axis at 45°, 30°, and 0° relative to the horizontal axis, respectively, while the half-wave plate (HWP) always sets the fast axis at 0° relative to the horizontal axis. Evidence of coherence transfer and the effectiveness of $\mathcal{E}_{\mathrm{V}}$ in four-photon and six-photon networks is shown in Figs. 4(d) and 4(e), respectively. Here, the measurement results are minimized relative to those from $\mathcal{E}_{\mathcal{I}}$ by using SDP [40–43] to derive $\mathcal{Q}$. The ideal value of $\mathcal{Q}$ is shown by the gray solid line, while the experimentally measured value is depicted by the yellow bar. The difference between the ideal and experimental values primarily arises from limited state fidelity and photonic-fusion errors. See Supplemental Material [40] for details, including the relationship between criterion (1) and the witness for genuine multipartite entanglement.

Similarly, in faithful one-qubit coherence transfer, we first establish coherence and then transfer it via remote state preparation [54,55], wave plates, polarization measurements, and

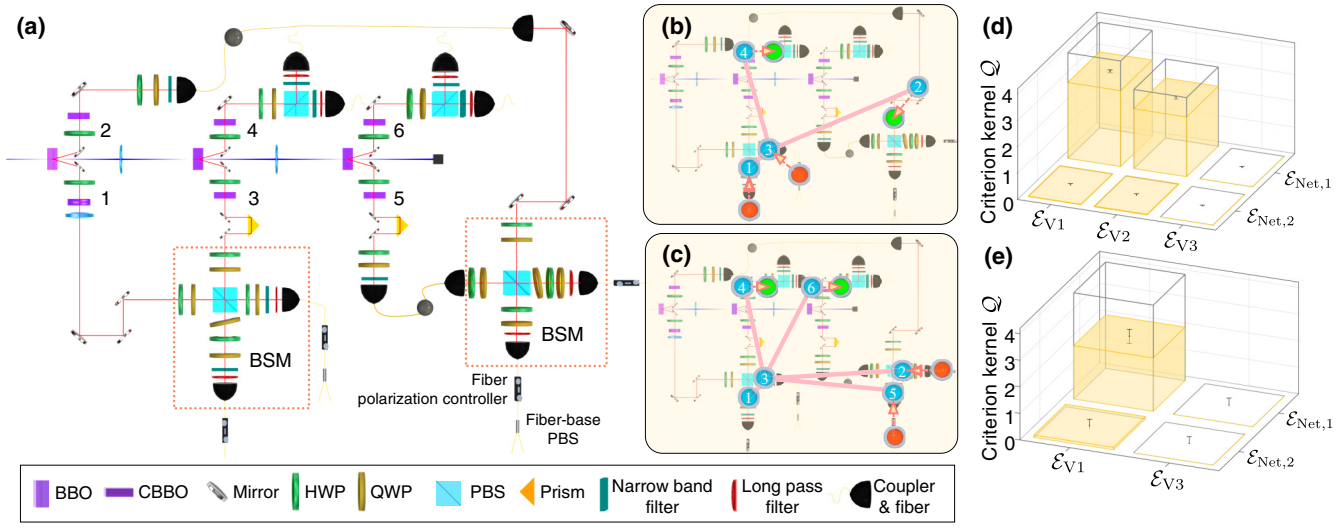



FIG. 4. Detection of experimental coherence transfer in multiphoton entanglement networks. (a) Experimental setup. The three spontaneous parametric down-conversion (SPDC) sources [33] are pumped by a pulsed laser beam. In each source, a β-barium-borate (BBO) crystal is pumped to generate pairs of polarization-entangled photons via type-II noncollinear SPDC, with walk-off compensation provided by an additional BBO crystal (CBBO). The three photon pairs prepared in modes 1–2, 3–4, and 5–6 are intended to generate the target state $|\psi^-\rangle = (1/\sqrt{2})(|HV\rangle - |VH\rangle)$, where $|H\rangle$ ($|V\rangle$) denotes the horizontal (vertical) photon polarization state. Combined with wave-plate sets, two photonic fusion units temporally and spatially overlap photon pairs at a PBS to perform either a photonic fusion operation [47,48] or a BSM [47,49]. The results can be considered as star multiphoton entanglement networks [Fig. 1(a)]. Two-qubit coherence transfer pathways in the four-photon and six-photon networks are shown in panels (b) and (c), respectively, with corresponding experimental detection results in panels (d) and (e), identified by criterion (1). See Supplemental Material [40] for the experimental details and results above.

shared entanglement, followed by photonic fusion operations to subsequent stage nodes. See Supplemental Material [40] for details.

Our proof-of-principle experiment demonstrates the first identification of coherence transfer using two measurement settings. While all photonic elements required to determine $\mathcal{Q}$ can, in principle, be calibrated, the criterion in Eq. (1) allows the elements for $\mathcal{E}_V$ to remain uncharacterized under the prescribed assumption [56]. This experimental demonstration helps clarify general quantum network scenarios in which uncharacterized situations can arise. In such cases, $\mathcal{E}_V$ is generally assumed to be uncharacterized or uncalibrated by default.

*Conclusion and outlook.* In this work, we have developed a general criterion for detecting coherence transfers in quantum networks under typical experimental constraints. It requires only two measurement settings, regardless of the network's size, even when checkpoint nodes are uncharacterized, and measures only a minimal one-network output, up to the number of output state dimensions. By identifying the coexistence of static and dynamic coherence, it is comprehensive and suitable for a wide range of coherence network detection tasks across different experimental access levels, from spatial to temporal, including entanglement, multicoherence sources, and quantum transport networks, compared with existing works. While existing methods have fallen short in assessing coherence under the experimental constraints, our experimentally derived values of the criterion kernel clearly demonstrate coherence transfer in the multiphoton entanglement networks we constructed. More generally, this fundamental yet practical framework helps explore coherence transfer in complex systems, such as transient coherences in photosynthetic systems, while accounting for practical constraints in 2DES.

*Acknowledgments.* We thank N. Lambert, F. Nori, G.-Y. Chen, Y.-N. Chen, H. Lu, Y.-A. Chen, and J.-W. Pan for their valuable discussions on coherence, which motivated our research from previous work [22] to this current study. We also appreciate J.-Y. Wu and C.-S. Chuu for their helpful feedback. This work was partially supported by the National Science and Technology Council, Taiwan, under Grants No. NSTC 114-2112-M-006-016-MY3, No. NSTC 114-2119-M-007-012, and No. NSTC 115-2119-M-007-004.

*Data availability*. The theoretical and experimental data supporting the findings of this work are available upon reasonable request from the authors.

[1] H. J. Kimble, The quantum internet, Nature (London) **453**, 1023 (2008).
[2] S. Wehner, D. Elkouss, and R. Hanson, Quantum internet: A vision for the road ahead, Science **362**, eaam9288 (2018).
[3] N. Lambert, Y.-N. Chen, Y.-C. Cheng, C.-M. Li, G.-Y. Chen, and F. Nori, Quantum biology, Nat. Phys. **9**, 10 (2013).
[4] P. Kómár, E. M. Kessler, M. Bishof, L. Jiang, A. S. Sørensen, J. Ye, and M. D. Lukin, A quantum network of clocks, Nat. Phys. **10**, 582 (2014).
[5] T. D. Ladd, F. Jelezko, R. Laflamme, Y. Nakamura, C. Monroe, and J. L. O'Brien, Quantum computers, Nature (London) **464**, 45 (2010).
[6] N. Gisin and R. Thew, Quantum communication, Nature Photon. **1**, 165 (2007).
[7] S. Ritter, C. Nölleke, C. Hahn, A. Reiserer, A. Neuzner, M. Uphoff, M. Mücke, E. Figueroa, J. Bochmann, and G. Rempe, An elementary quantum network of single atoms in optical cavities, Nature (London) **484**, 195 (2012).
[8] A. Streltsov, G. Adesso, and M. B. Plenio, *Colloquium*: Quantum coherence as a resource, Rev. Mod. Phys. **89**, 041003 (2017).
[9] G. Gour and A. Winter, How to quantify a dynamical quantum resource, Phys. Rev. Lett. **123**, 150401 (2019).
[10] Y. Liu and X. Yuan, Operational resource theory of quantum channels, Phys. Rev. Res. **2**, 012035 (2020).
[11] C.-C. Kuo, S.-H. Chen, W.-T. Lee, H.-M. Chen, H. Lu, and C.-M. Li, Quantum process capability, Sci. Rep. **9**, 20316 (2019).
[12] C. Couteau and S. Lazić, How to define quantum technology, Nat. Rev. Phys. **7**, 234 (2025).
[13] A. Jha, F. Zheng, Z. Liu, S. Mukamel, M. Thorwart, R. J. D. Miller, and H.-G. Duan, Quantum coherent dynamics in photosynthetic protein complexes, Chem. Soc. Rev. **55**, 1089 (2026).
[14] N. Lambert, C. Emary, Y.-N. Chen, and F. Nori, Distinguishing quantum and classical transport through nanostructures, Phys. Rev. Lett. **105**, 176801 (2010).
[15] D. N. Biggerstaff, R. Heilmann, A. A. Zecevik, M. Gräfe, M. A. Broome, A. Fedrizzi, S. Nolte, A. Szameit, A. G. White, and I. Kassal, Enhancing coherent transport in a photonic network using controllable decoherence, Nat. Commun. **7**, 11282 (2016).
[16] C.-Y. Lu, Y. Cao, C.-Z. Peng, and J.-W. Pan, Micius quantum experiments in space, Rev. Mod. Phys. **94**, 035001 (2022).
[17] Y. Li, W.-Q. Cai, J.-G. Ren, C.-Z. Wang, M. Yang, L. Zhang, H.-Y. Wu, L. Chang, J.-C. Wu, B. Jin, *et al.*, Microsatellite-based real-time quantum key distribution, Nature (London) **640**, 47 (2025).
[18] T. Brandes, Coherent and collective quantum optical effects in mesoscopic systems, Phys. Rep. **408**, 315 (2005).
[19] J. Yuen-Zhou, J. J. Krich, M. Mohseni, and A. Aspuru-Guzik, Quantum state and process tomography of energy transfer systems via ultrafast spectroscopy, Proc. Natl. Acad. Sci. USA **108**, 17615 (2011).
[20] E. Collini, 2D electronic spectroscopic techniques for quantum technology applications, J. Phys. Chem. C **125**, 13096 (2021).
[21] T. Baumgratz, M. Cramer, and M. B. Plenio, Quantifying coherence, Phys. Rev. Lett. **113**, 140401 (2014).
[22] C.-M. Li, N. Lambert, Y.-N. Chen, G.-Y. Chen, and F. Nori, Witnessing quantum coherence: From solid-state to biological systems, Sci. Rep. **2**, 885 (2012).
[23] J. Kofler and C. Brukner, Condition for macroscopic realism beyond the Leggett-Garg inequalities, Phys. Rev. A **87**, 052115 (2013).
[24] C. Napoli, T. R. Bromley, M. Cianciaruso, M. Piani, N. Johnston, and G. Adesso, Robustness of coherence: An operational and observable measure of quantum coherence, Phys. Rev. Lett. **116**, 150502 (2016).

[25] M. Piani, M. Cianciaruso, T. R. Bromley, C. Napoli, N. Johnston, and G. Adesso, Robustness of asymmetry and coherence of quantum states, Phys. Rev. A **93**, 042107 (2016).

[26] W. Zheng, Z. Ma, H. Wang, S.-M. Fei, and X. Peng, Experimental demonstration of observability and operability of robustness of coherence, Phys. Rev. Lett. **120**, 230504 (2018).

[27] Z. Ma, Z. Zhang, Y. Dai, Y. Dong, and C. Zhang, Detecting and estimating coherence based on coherence witnesses, Phys. Rev. A **103**, 012409 (2021).

[28] M.-S. Li, W. Xu, S.-M. Fei, Z.-J. Zheng, and Y.-L. Wang, Witnessing quantum coherence with prior knowledge of observables, Phys. Rev. A **109**, 032422 (2024).

[29] A. J. Leggett and A. Garg, Quantum mechanics versus macroscopic realism: Is the flux there when nobody looks? Phys. Rev. Lett. **54**, 857 (1985).

[30] G. C. Knee, S. Simmons, E. M. Gauger, J. J. L. Morton, H. Riemann, N. V. Abrosimov, P. Becker, H.-J. Pohl, K. M. Itoh, M. L. W. Thewalt, G. A. D. Briggs, and S. C. Benjamin, Violation of a Leggett–Garg inequality with ideal non-invasive measurements, Nat. Commun. **3**, 606 (2012).

[31] Y.-Q. Nie, H. Zhou, J.-Y. Guan, Q. Zhang, X. Ma, J. Zhang, and J.-W. Pan, Quantum coherence witness with untrusted measurement devices, Phys. Rev. Lett. **123**, 090502 (2019).

[32] F. Bibak, F. Del Santo, and B. Dakić, Quantum coherence in networks, Phys. Rev. Lett. **133**, 230201 (2024).

[33] J.-W. Pan, Z.-B. Chen, C.-Y. Lu, H. Weinfurter, A. Zeilinger, and M. Żukowski, Multiphoton entanglement and interferometry, Rev. Mod. Phys. **84**, 777 (2012).

[34] M. Pompili, S. L. N. Hermans, S. Baier, H. K. C. Beukers, P. C. Humphreys, R. N. Schouten, R. F. L. Vermeulen, M. J. Tiggelman, L. dos Santos Martins, B. Dirkse, S. Wehner, and R. Hanson, Realization of a multinode quantum network of remote solid-state qubits, Science **372**, 259 (2021).

[35] D. Awschalom, K. K. Berggren, H. Bernien, S. Bhave, L. D. Carr, P. Davids, S. E. Economou, D. Englund, A. Faraon, M. Fejer, *et al.*, Development of quantum interconnects (QuICs) for next-generation information technologies, PRX Quantum **2**, 017002 (2021).

[36] R. Raussendorf, D. E. Browne, and H. J. Briegel, Measurement-based quantum computation on cluster states, Phys. Rev. A **68**, 022312 (2003).

[37] S. Barz, E. Kashefi, A. Broadbent, J. F. Fitzsimons, A. Zeilinger, and P. Walther, Demonstration of blind quantum computing, Science **335**, 303 (2012).

[38] C. M. Knaut, A. Suleymanzade, Y.-C. Wei, D. R. Assumpcao, P.-J. Stas, Y. Q. Huan, B. Machielse, E. N. Knall, M. Sutula, G. Baranes, N. Sinclair, C. De-Eknamkul, D. S. Levonian, M. K. Bhaskar, H. Park, M. Lončar, and M. D. Lukin, Entanglement of nanophotonic quantum memory nodes in a telecom network, Nature (London) **629**, 573 (2024).

[39] The cost includes all experimental overhead required to ultimately determine $\mathcal{E}_{\mathrm{V}}$, such as preparing complementary input states and performing full state and process tomography. If characterizing $\mathcal{E}_{\mathrm{V}}$ is infeasible or the network end node cannot provide the cost, the checkpoint node cannot consider $\mathcal{E}_{\mathrm{V}}$ as characterized and therefore cannot perform the subsequent check of whether $\mathcal{E}_{\mathrm{Net}}$ preserves coherence.

[40] See Supplemental Material at http://link.aps.org/supplemental/10.1103/lv5x-mvvh for the criterion's generality regarding input and output state settings, a proof and an example for detecting coherence dynamics in the time domain, details of coherence-transfer experiments in multiphoton entanglement networks, and a description of how these experiments illustrate key aspects of coherence transfer in entanglement networks, which includes Refs. [57–68].

[41] J. Lofberg, YALMIP: A toolbox for modeling and optimization in MATLAB, in *2004 IEEE International Conference on Robotics and Automation (IEEE Cat. No. 04CH37508)* (IEEE, Piscataway, New Jersey, 2004), pp. 284–289.

[42] K. C. Toh, M. J. Todd, and R. H. Tütüncü, SDPT3—A MATLAB software package for semidefinite programming, version 1.3, Optim. Methods Software **11**, 545 (1999).

[43] E. D. Andersen and K. D. Andersen, The MOSEK interior point optimizer for linear programming: An implementation of the homogeneous algorithm, in *High Performance Optimization*, edited by H. Frenk, K. Roos, T. Terlaky, and S. Zhang (Springer, 2000), pp. 197–232.

[44] Both the concept of two coherences coexisting, underlying Eq. (1), and the criterion itself are novel. Therefore, our result addresses a clear gap in the literature on the practical verification of quantum resources in large-scale, noisy, or partially accessible networks. This clearly distinguishes our framework for $\mathcal{Q}$ from other coherence measures or witnesses cited in the main text, particularly in how $\mathcal{Q}$ relates to existing methods. We compare $\mathcal{Q}$ with the kernel of the measurement-device-independent coherence witness [31], which aims to detect coherence even with uncharacterized measurement devices. Fully characterizing an uncharacterized positive operator-valued measure requires measurement-device tomography (MDT), which poses experimental challenges in quantum networks. In contrast, determining $\mathcal{Q}$ does not require MDT overhead.

[45] I. L. Chuang and M. A. Nielsen, Prescription for experimental determination of the dynamics of a quantum black box, J. Mod. Opt. **44**, 2455 (1997).

[46] The introduced criterion can also be rephrased as a direct *composition principle* under the assumed characterization of $\mathcal{E}_{\mathrm{V}}$ as having coherence-creation capability: If $\mathcal{E}_{\mathrm{Net}}$ preserves or transfers the relevant basis coherence to the output, then a downstream coherence-to-population analyzer $\mathcal{E}_{\mathrm{V}}$ can reveal it in populations.

[47] J.-W. Pan and A. Zeilinger, Greenberger-Horne-Zeilinger-state analyzer, Phys. Rev. A **57**, 2208 (1998).

[48] C.-Y. Lu, X.-Q. Zhou, O. Gühne, W.-B. Gao, J. Zhang, Z.-S. Yuan, A. Goebel, T. Yang, and J.-W. Pan, Experimental entanglement of six photons in graph states, Nat. Phys. **3**, 91 (2007).

[49] D. Bouwmeester, J.-W. Pan, K. Mattle, M. Eibl, H. Weinfurter, and A. Zeilinger, Experimental quantum teleportation, Nature (London) **390**, 575 (1997).

[50] H.-P. Breuer, E.-M. Laine, J. Piilo, and B. Vacchini, *Colloquium*: Non-Markovian dynamics in open quantum systems, Rev. Mod. Phys. **88**, 021002 (2016).

[51] W.-T. Kao, C.-Y. Huang, T.-J. Tsai, S.-H. Chen, S.-Y. Sun, Y.-C. Li, T.-L. Liao, C.-S. Chuu, H. Lu, and C.-M. Li, Scalable determination of multipartite entanglement in quantum networks, npj Quantum Inf. **10**, 73 (2024).

[52] M. Żukowski, A. Zeilinger, M. A. Horne, and A. K. Ekert, "Event-ready-detectors" Bell experiment via entanglement swapping, Phys. Rev. Lett. **71**, 4287 (1993).

[53] J.-W. Pan, D. Bouwmeester, H. Weinfurter, and A. Zeilinger, Experimental entanglement swapping: Entangling photons that never interacted, Phys. Rev. Lett. **80**, 3891 (1998).

[54] C. H. Bennett, D. P. DiVincenzo, P. W. Shor, J. A. Smolin, B. M. Terhal, and W. K. Wootters, Remote state preparation, Phys. Rev. Lett. **87**, 077902 (2001).

[55] S.-H. Chen, C. Hsu, Y.-C. Kao, B.-Y. Lee, Y.-S. Liu, Y.-N. Chen, and C.-M. Li, Preparing remote states for genuine quantum networks, Commun. Phys. **7**, 352 (2024).

[56] It is worth noting that "output coherence witnessed through $\mathcal{E}_{\mathrm{V}}$" can differ from "coherence transfer through the network." Their consistency depends on whether the entire quantum network experiment and its output-state inspection satisfy the assumptions of our coherence-detection framework [Eq. (1)], excluding inconsistencies arising from actual coherence generation during the transfer stage, postselection artifacts in population measurements, or other model-dependent explanations.

[57] T. Fujisawa, T. Hayashi, R. Tomita, and Y. Hirayama, Bidirectional counting of single electrons, Science **312**, 1634 (2006).

[58] D. M. Greenberger, M. A. Horne, and A. Zeilinger, Going beyond Bell's theorem, in *Bell's Theorem, Quantum Theory, and Conceptions of the Universe*, edited by M. Kafatos (Kluwer, Dordrecht, 1989), pp. 67–72.

[59] P. G. Kwiat, K. Mattle, H. Weinfurter, A. Zeilinger, A. V. Sergienko, and Y. Shih, New high-intensity source of polarization-entangled photon pairs, Phys. Rev. Lett. **75**, 4337 (1995).

[60] D.-G. Im, Y. Kim, and Y.-H. Kim, Dispersion cancellation in a quantum interferometer with independent single photons, Opt. Express **29**, 2348 (2021).

[61] G. Tóth and O. Gühne, Detecting genuine multipartite entanglement with two local measurements, Phys. Rev. Lett. **94**, 060501 (2005).

[62] A. K. Pati, Minimum classical bit for remote preparation and measurement of a qubit, Phys. Rev. A **63**, 014302 (2000).

[63] J.-W. Pan, C. Simon, Č. Brukner, and A. Zeilinger, Entanglement purification for quantum communication, Nature (London) **410**, 1067 (2001).

[64] J.-W. Pan, S. Gasparoni, R. Ursin, G. Weihs, and A. Zeilinger, Experimental entanglement purification of arbitrary unknown states, Nature (London) **423**, 417 (2003).

[65] X.-L. Wang, L.-K. Chen, W. Li, H.-L. Huang, C. Liu, C. Chen, Y.-H. Luo, Z.-E. Su, D. Wu, Z.-D. Li, H. Lu, Y. Hu, X. Jiang, C.-Z. Peng, L. Li, N.-L. Liu, Y.-A. Chen, C.-Y. Lu, and J.-W. Pan, Experimental ten-photon entanglement, Phys. Rev. Lett. **117**, 210502 (2016).

[66] H.-S. Zhong, Y. Li, W. Li, L.-C. Peng, Z.-E. Su, Y. Hu, Y.-M. He, X. Ding, W. Zhang, H. Li, L. Zhang, Z. Wang, L. You, X.-L. Wang, X. Jiang, L. Li, Y.-A. Chen, N.-L. Liu, C.-Y. Lu, and J.-W. Pan, 12-photon entanglement and scalable scattershot boson sampling with optimal entangled-photon pairs from parametric down-conversion, Phys. Rev. Lett. **121**, 250505 (2018).

[67] B. Bell, A. S. Clark, M. S. Tame, M. Halder, J. Fulconis, W. J. Wadsworth, and J. G. Rarity, Experimental characterization of photonic fusion using fiber sources, New J. Phys. **14**, 023021 (2012).

[68] D. E. Browne and T. Rudolph, Resource-efficient linear optical quantum computation, Phys. Rev. Lett. **95**, 010501 (2005).